Published in final edited form as:

Nature. 2009 February 12; 457(7231): 887–891. doi:10.1038/nature07619.

Runx1 is required for the endothelial to hematopoietic cell transition but not thereafter

Michael J. Chen[1,2,4], **Tomomasa Yokomizo**[3], **Brandon Zeigler**[1], **Elaine Dzierzak**[3], and **Nancy A. Speck**[1,3,4,5]

[1]Department of Biochemistry, Dartmouth Medical School, Hanover NH 03755 [2]Department of Genetics, Dartmouth Medical School, Hanover NH 03755 [3]Department of Cell Biology and Genetics, Erasmus University, Rotterdam, the Netherlands

Abstract

HSCs are the founder cells of the adult hematopoietic system, and thus knowledge of the molecular program directing their generation during development is important for regenerative hematopoietic strategies. Runx1 is a pivotal transcription factor required for HSC generation in the vascular regions of the mouse conceptus - the aorta, vitelline and umbilical arteries, yolk sac and placenta 1, 2. It is thought that HSCs emerge from vascular endothelial cells through the formation of intra-arterial clusters 3 and that Runx1 functions during the transition from 'hemogenic endothelium' to HSCs 4, 5. Here we show by conditional deletion that Runx1 activity in vascular endothelial cadherin (VEC) positive endothelial cells is indeed essential for intra-arterial cluster, hematopoietic progenitor, and HSC formation. In contrast, Runx1 is not required in cells expressing Vav, one of the first pan-hematopoietic genes expressed in HSCs. Collectively these data show that Runx1 function is essential in endothelial cells for hematopoietic progenitor and HSC formation from the vasculature, but its requirement ends once or before Vav is expressed.

HSCs are found in several independent sites in the conceptus, and the transcription factor Runx1, which is required for HSC generation, is expressed in these sites 4. Runx1 protein is seen in the mesodermal masses and endoderm of the prospective yolk sac blood islands at the neural plate stage 4, 6, in mesoderm of the distal allantois and chorion (precursors of the placenta) at headfold stages 7, and in endothelial cells in the distal allantois, dorsal aorta, vitelline and umbilical arteries starting the 4–6 somite pair (s) stage (data not shown). Runx1 is expressed at 9.5–10.5 days post coitus (dpc) in both endothelial and mesenchymal cells in the dorsal aorta and placental labyrinth 4, 7, 8. Therefore it is not clear whether Runx1 is required in mesoderm, endoderm, mesenchyme, and/or endothelial cells for intra-arterial cluster and HSC formation.

[5]Corresponding author: Nancy A. Speck, Phone: 215-898-0247, nancyas@exchange.upenn.edu.
[4]Current address: Abramson Family Cancer Research Institute and Department of Cell and Developmental Biology, University of Pennsylvania School of Medicine, Philadelphia, PA 19104

To examine the hypothesis that Runx1 is required in endothelial cells *per se* we deleted *Runx1* in VEC positive cells. VEC is a transmembrane protein located at cell-to-cell adherens junctions that is involved in endothelial cell adhesion 9. VEC is expressed transiently in the yolk sac mesoderm at 7.5 dpc, however at 8.5 dpc its expression is highly restricted to endothelial cells in the dorsal aorta and heart 10–12. At 9.5 dpc VEC is expressed in vasculature throughout the conceptus 11. Distinct mesodermal populations give rise to the yolk sac blood islands and to the major arteries of the conceptus, including those in the placenta 13–15. Thus with VEC-Cre we could monitor the impact of Runx1 excision on HSC formation from the vasculature including the dorsal aorta, vitelline and umbilical arteries, and placenta - sites where VEC expression initiates in endothelium.

We generated a VEC-Cre transgene (Fig. 1a) and used *R26R-lacZ* and *R26R-YFP* reporter mice to characterize its activity. The first sites of VEC-Cre activity were in the yolk sac and chorionic mesoderm (not shown). Primitive erythrocytes in the yolk sac blood islands were β-gal$^+$, as were PECAM1$^+$ cells in the vitelline vasculature (Fig. 1b). By 9.5 dpc β-gal activity was high in vasculature throughout the conceptus (Fig. 1c), particularly within PECAM1$^+$ cells in the developing labyrinth of the placenta and in the umbilical artery (Fig. 1d). At 10.5 dpc β-gal$^+$ endothelial cells and intra-arterial clusters were present in the dorsal aorta, vitelline and umbilical arteries, whereas mesenchymal cells were β-gal$^-$ (Fig. 1f). VEC-Cre mediated excision occurred in 77% (± 11%) of cell surface Sca1$^-$ VEC$^+$ endothelial cells in the AGM region plus vitelline and umbilical arteries (AGM+V+U) of 11.5 dpc conceptuses and in 86% of Sca1$^+$ VEC$^+$ cells (Fig. 1e) (Sca-1 marks 50% of HSCs, and VEC marks all HSCs in the AGM region) 2, 16. No excision was detectable in Sca1$^+$ VEC$^-$ cells (Fig. 1e). There was widespread VEC-Cre activity in the fetal liver (Fig. 1f,g), 99% of which was localized to CD45$^+$, CD71$^+$, and/or Ter119$^+$ blood cells in *R26R-YFP;VEC-Cre* conceptuses (not shown). Approximately 85% of fetal liver blood cells in 15.5 dpc *R26R-YFP;VEC-Cre* fetuses were YFP$^+$ (Fig, 1h), and are consequently derived from cells that at one time in their history expressed VEC. Ninety six percent of CD45$^+$ adult bone marrow cells were YFP$^+$ (Fig. 1i), and thus almost all adult blood is derived from VEC-expressing cells.

VEC-Cre mediated Runx1 deletion caused a 65% rate of fetal lethality (Supplementary Table 1), and approximately 10% of 12.5 dpc *Runx1$^{f/f}$; VEC-cre* fetuses had central nervous system hemorrhaging and fetal liver anemia characteristic of Runx1 deficiency 17, 18 (Fig. 2a and Supplementary Table 1). There was an 8-fold decrease in c-kit$^+$ cells in the livers of 11.5 dpc *Runx1$^{f/f}$; VEC-cre* fetuses (Fig. 2b), and in colony-forming unit culture (CFU-C) progenitors in all hematopoietic sites (Fig. 2c). DNA analysis revealed that 84% of colonies derived from *Runx1$^{f/+}$;VEC-Cre* fetal cells had excised the *Runx1^f* allele (Fig. 2d and Supplementary Table 2), consistent with the deletion efficiency determined with the *R26R-YFP* allele. In contrast, only one out of 389 colonies picked from cultures established from *Runx1$^{f/f}$;VEC-cre* fetuses had two deleted *Runx1^f* alleles. Thus, at least one functional *Runx1* allele must be present in a VEC$^+$ cell for CFU-C progenitors to emerge in the fetus.

In vivo repopulation assays revealed that hematopoietic tissues of 11.5 dpc *Runx1$^{f/f}$;VEC-Cre* conceptuses could engraft adult mice, but at a much reduced frequency as compared to *Runx1$^{f/+}$;VEC-cre* cells (Fig. 3a,b). While all donor-derived CFU-C progenitors in the

recipients of *Runx1*$^{f/+}$*;VEC-Cre* HSCs had a deleted *Runx1*^{f} allele, both *Runx1*^{f} alleles were deleted in only one out of 192 colonies generated from *Runx1*$^{f/f}$*;VEC-Cre* donor-derived HSCs (Fig. 3c). We also analyzed the bone marrow of viable *Runx1*$^{f/f}$*;VEC-Cre* adult mice and found that all colonies retained at least one undeleted *Runx1*^{f} allele (Supplementary Table 2). Therefore there is strong selective pressure for cells that escape the excision of at least one *Runx1*^{f} allele to contribute to hematopoiesis in *Runx1*$^{f/f}$*;VEC-Cre* mice. Together these data indicate that Runx1 is required in VEC^{+} cells for HSC formation.

As the autonomous production of HSCs occurs first in the major arteries of the conceptus at 10.5 dpc (dorsal aorta, vitelline and umbilical) 19, and HSCs localize to the walls of these arteries 2, 16, we examined intra-arterial cluster formation in *Runx1*$^{f/f}$*;VEC-Cre* embryos. VEC is expressed on both endothelial cells and intra-arterial clusters, but the first potential site of deletion is in the endothelium that gives rise to the clusters. No hematopoietic clusters were visible in the dorsal aorta, vitelline and umbilical arteries of *Runx1*$^{f/f}$*;VEC-Cre* animals, and there was a 90-fold decrease in c-kit^{hi} cells (Fig. 3d).Thus, the important deletion event in these arteries occurred in the endothelium.

To confirm this and to determine whether Runx1 continues to be required once the endothelial to HSC transition is complete, we examined the outcome of deleting *Runx1* with Vav-Cre. Vav1 is a GDP/GTP nucleotide exchange factor for Rho/Rac, whose expression is restricted to hematopoietic cells 20, 21. *Vav1* was also implicated as a Runx1 target, as its transcript was not detected in the AGM region or fetal liver of Runx1 deficient embryos 22. Excision of the *R26R-YFP* allele by Vav-Cre occurred in 68% (±16%) of CD45^{+}VEC^{-} hematopoietic cells from the AGM region, vitelline and umbilical arteries and not in CD45^{-}VEC^{+} endothelium (Fig. 4a). Excised (β-gal^{+}) cells were not found in intra-arterial clusters at either 10.5 or 11.5 dpc, and were instead located within the sub-aortic mesenchyme and the circulation (Fig. 4b–d). Therefore Vav-Cre marked cells that either originated in the yolk sac, or had upregulated Vav-Cre subsequent to their release from the intra-arterial clusters. β-gal^{+} cells were detectable in the fetal liver at 10.5 dpc (not shown), and by 11.5 dpc 63% (±13%) of CD45^{+}VEC^{-} cells in the fetal liver were YFP^{+} (Fig. 4a) and were easily seen by histology (Fig. 4e). Fetal liver HSCs transiently express cell surface VEC 23, 24. Sixty three (±15) percent of the CD45^{+}VEC^{+} HSC-containing population in the 11.5 dpc fetal liver was YFP^{+} (Fig. 4a), and by 15.5 dpc 90% of lineage negative Sca1^{+} Mac1^{+} fetal liver cells were YFP^{+} (not shown), similar to the excision frequencies reported previously 21. Thus with Vav-Cre we could execute an excision in CD45^{+} cells while avoiding deletion in the intra-arterial clusters or endothelium.

In contrast to VEC-Cre, excision of *Runx1* with Vav-Cre did not affect fetal or adult viability (Supplementary Table 3). The hematopoietic deficiencies described in adult mice upon Runx1 deletion with Mx1-Cre, including thrombocytopenia, defective lymphopoiesis, and expansion of the lineage negative (Lin^{-}) Sca-1^{+} c-kit^{+} population 25, 26 were also apparent in the Vav-Cre deleted mice (Supplementary Figure 2). Fetal livers from 15.5 dpc *Runx1*$^{f/f}$*;Vav-Cre* mice had *increased* numbers of CFU-C progenitors, particularly granulocyte/macrophage (GM) and multipotent (GEMM) progenitors (Fig. 4f), as was previously observed in the bone marrow of Mx1-Cre deleted adult mice 25, 26. Thus deletion of Runx1 in Vav^{+} cells did not impair the emergence of CFU-C progenitors but did

affect their homeostasis. Importantly, both *Runx1*^{f} alleles were deleted in 280/281 colonies from 15.5 dpc *Runx1*$^{f/f}$*;Vav-Cre* fetal livers (Supplementary Table 4). Colonies from 11.5 dpc animals contained *Runx1*^{f} alleles at various stages of deletion (Fig. 4g) since excision is initiating close to that time. However, 32% of colonies from the hematopoietic tissues of 11.5 dpc fetuses contained two deleted *Runx1*^{f} alleles, and by 14.5 dpc 100% of fetal liver progenitors had deleted both alleles (Supplementary Table 4). We therefore conclude that Runx1 function is no longer required once a CFU-C progenitor expresses Vav.

Mice were efficiently engrafted with hematopoietic tissues from 11.5 dpc *Runx1*$^{f/f}$*;Vav-Cre* conceptuses (Fig. 4h), and in all colonies (94/94) derived from donor *Runx1*$^{f/f}$*;Vav-Cre* HSCs, both *Runx1*^{f} alleles were deleted (Supplementary Table 4). The same was true in adult *Runx1*$^{f/f}$*;Vav-Cre* mice – virtually all CFU-C progenitors had deleted both *Runx1*^{f} alleles (Supplementary Table 4). Hence, Runx1 is not required in a Vav^{+} HSC.

In summary, the most essential function of Runx1 is during the transition from VEC^{+} cells to Vav^{+} HSCs, although it continues to provide important activity in maintaining normal HSC function and for the terminal differentiation of some lineages 25, 26 (Supplementary Figure 1). Our data demonstrate that the relevant VEC^{+} HSC precursors are in the hemogenic endothelium. Although the yolk sac mesoderm expresses VEC, in the placenta, vitelline and umbilical arteries, and dorsal aorta, which are independent hematopoietic sites derived from distinct populations of mesoderm 13–15, VEC expression is restricted to intra-arterial clusters and endothelium. Intra-arterial clusters in these sites are absent in *Runx1*$^{f/f}$*;VEC-Cre* conceptuses, and therefore the relevant deletion event must have occurred in the endothelium from which they are derived. Continued deletion by VEC-Cre in fetal liver HSCs is unlikely because Runx1 is no longer required once HSCs reach the fetal liver and express Vav, yet they all contain undeleted *Runx1*^{f} alleles.

We also showed that most adult blood (≥ 95%) is derived from a cell that at one time in its history expressed VEC. Our working model is that most HSCs are born from VEC^{+} hemogenic endothelium in the conceptus, although a VEC^{+} HSC precursor in adult bone marrow cannot be ruled out. Monvoisin et al. 27 found that a small but detectable number of bone marrow cells (< 0.4%) could be labeled when a tamoxifen-regulated VEC-Cre was activated in the adult, hence VEC^{+} adult HSC precursors, if they exist, are rare cells.

Another model for HSC emergence posits that HSCs in the AGM region originate in subaortic patches of cells (SAPs) in the ventral para-aortic mesenchyme of the dorsal aorta 28, and migrate toward the aorta and between endothelial cells to form the intra-aortic clusters. As we showed that almost all blood is derived from VEC^{+} cells, SAP cells must upregulate VEC as they protrude through the endothelium.

Methods

Conditional deletion by VEC-Cre or Vav-Cre

A 2.5 kb VEC promoter sequence was cloned between insulators from the chicken γ-globin gene 29 and used to drive Cre expression. The construct was injected into fertilized oocytes from C57BL6/J x 129S1/SvImJ F1 mice. *R26R-lacZ/+;VEC-Cre* or *R26R-YFP/+;VEC-Cre*

conceptuses were generated by crossing *VEC-Cre*/+ males with *R26R-lacZ*/+ or *R26R-YFP*/+ females. *Runx1$^{f/+}$;VEC-Cre* and *Runx1$^{f/f}$;VEC-Cre* conceptuses were generated by crossing *Runx1$^{f/+}$; VEC-Cre*/+ males with *Runx1$^{f/f}$* females. *Runx1$^{f/+}$;R26R-YFP/+;VEC-Cre or Runx1$^{f/f}$;R26R-YFP/+;VEC-Cre* conceptuses were generated from crossing *Runx1$^{f/+}$;R26R-YFP/+; VEC-Cre*/+ males with *Runx1$^{f/f}$* females. Similar breeding strategies were employed for Vav-Cre deletion.

Microscopic and histological analyses

Conceptuses were suspended in phosphate-buffered saline or in a 1:2 mixture of benzyl alcohol/benzyl benzoate and visualized with a stereomicroscope. X-gal (Sigma) staining was performed as described previously 4. In some cases the conceptuses were also incubated with rat anti-mouse Pecam1 and ABC reagent at 4°C 30, then treated with DAB peroxidase substrate. Conceptuses were embedded in paraffin, sectioned, and counterstained with nuclear fast red.

To analyze intra-aortic clusters, embryos were fixed and stained with anti-c-Kit and anti-PECAM1-antibodies. A 1:2 mix of benzyl alcohol/benzyl benzoate was used to increase the transparency of tissues. Samples were analyzed with a confocal microscope using the multi track sequential mode. Three-dimensional reconstructions were generated from Z-stacks (62–87 serial sections).

Hematopoietic assays

Methylcellulose colony forming assays were performed as described previously 4 and colonies counted after 7 days. Fetal tissues were transplanted as previously described 16.

Immuno-staining was performed with phycoerytherin, allophycocyanin, or Alexa Fluor 647 conjugated antibodies Stained cells were analyzed on a Becton Dickinson FACSCalibur flow cytometer. Dead cells were excluded with 7AAD.

Supplementary Material

Refer to Web version on PubMed Central for supplementary material.

Acknowledgments

The authors thank Gary Ward for his assistance with flow, Thomas Graf for the Vav-Cre mice, and Philippe Huber for the VEC regulatory sequences. This work was supported by R01HL091724 (NAS), R01DK54077 (ED), and T32 AI-07519 (BMZ). Core services were supported in part by the Norris Cotton Cancer Center (NIH CA23108) and the Abramson Family Cancer Research Institute.

Tomomasa Yokomizo performed the experiments in Figure 3d.

Brandon Zeigler performed the experiments in Figures 1b and 1d.

Michael Chen performed all the remaining experiments.

Elaine Dzierzak participated in the interpretation of the experiments and writing the manuscript.

Nancy A. Speck participated in the design and interpretation of the experiments, wrote the manuscript, and made the figures.

References

1. Cai Z, et al. Haploinsufficiency of AML1/CBFA2 affects the embryonic generation of mouse hematopoietic stem cells. Immunity. 2000; 13:423–431. [PubMed: 11070161]
2. North TE, et al. Runx1 expression marks long-term repopulating hematopoietic stem cells in the midgestation mouse embryo. Immunity. 2002; 16:661–672. [PubMed: 12049718]
3. Jaffredo T, Gautier R, Eichmann A, Dieterlen-Lièvre F. Intraaortic hemopoietic cells are derived from endothelial cells during ontogeny. Development. 1998; 125:4575–4583. [PubMed: 9778515]
4. North TE, et al. *Cbfa2* is required for the formation of intra-aortic hematopoietic clusters. Development. 1999; 126:2563–2575. [PubMed: 10226014]
5. Yokomizo T, et al. Requirement of Runx1/AML1/PEBP2αB for the generation of haematopoietic cells from endothelial cells. Genes Cells. 2001; 6:13–23. [PubMed: 11168593]
6. Samokhvalov IM, Samokhvalova NI, Nishikawa SI. Cell tracing shows the contribution of the yolk sac to adult haematopoiesis. Nature. 2007; 446:1056–1061. [PubMed: 17377529]
7. Zeigler BM, et al. The allantois and chorion, when isolated before circulation or chorio-allantoic fusion, have hematopoietic potential. Development. 2006; 133:4183–4192. [PubMed: 17038514]
8. Rhodes KE, et al. The emergence of hematopoietic stem cells is initiated in the placental vasculature in the absence of circulation. Cell Stem Cell. 2008; 2:252–263. [PubMed: 18371450]
9. Lampugnani MG, et al. The molecular organization of endothelial cell to cell junctions: differential association of plakoglobin, beta-catenin, and alpha-catenin with vascular endothelial cadherin (VE-cadherin). J Cell Biol. 1995; 129:203–217. [PubMed: 7698986]
10. Breier G, et al. Molecular cloning and expression of murine vascular endothelial-cadherin in early stage development of cardiovascular system. Blood. 1996; 87:630–641. [PubMed: 8555485]
11. Drake CJ, Fleming PA. Vasculogenesis in the day 6.5 to 9.5 mouse embryo. Blood. 2000; 95:1671–1679. [PubMed: 10688823]
12. Yokomizo T, et al. Characterization of GATA-1(+) hemangioblastic cells in the mouse embryo. Embo J. 2007; 26:184–196. [PubMed: 17159898]
13. Kinder SJ, et al. The orderly allocation of mesodermal cells to the extraembryonic structures and the anteroposterior axis during gastrulation of the mouse embryo. Development. 1999; 126:4691–4701. [PubMed: 10518487]
14. Lawson KA, Meneses JJ, Pedersen RA. Clonal analysis of epiblast fate during germ layer formation in the mouse embryo. Development. 1991; 113:891–911. [PubMed: 1821858]
15. Downs KM, Hellman ER, McHugh J, Barrickman K, Inman KE. Investigation into a role for the primitive streak in development of the murine allantois. Development. 2004; 131:37–55. [PubMed: 14645124]
16. de Bruijn M, et al. Hematopoietic stem cells localize to the endothelial cell layer in the midgestation mouse aorta. Immunity. 2002; 16:673–683. [PubMed: 12049719]
17. Okuda T, van Deursen J, Hiebert SW, Grosveld G, Downing JR. AML1, the target of multiple chromosomal translocations in human leukemia, is essential for normal fetal liver hematopoiesis. Cell. 1996; 84:321–330. [PubMed: 8565077]
18. Wang Q, et al. Disruption of the *Cbfa2* gene causes necrosis and hemorrhaging in the central nervous system and blocks definitive hematopoiesis. Proc. Natl. Acad. Sci. USA. 1996; 93:3444–3449.
19. de Bruijn MFTR, Speck NA, Peeters MCE, Dzierzak E. Definitive hematopoietic stem cells first emerge from the major arterial regions of the mouse embryo. EMBO J. 2000; 19:2465–2474. [PubMed: 10835345]
20. Ogilvy S, et al. Promoter elements of vav drive transgene expression in vivo throughout the hematopoietic compartment. Blood. 1999; 94:1855–1863. [PubMed: 10477714]
21. Stadtfeld M, Graf T. Assessing the role of hematopoietic plasticity for endothelial and hepatocyte development by non-invasive lineage tracing. Development. 2005; 132:203–213. [PubMed: 15576407]
22. Okada H, et al. AML1(−/−) embryos do not express certain hematopoiesis-related gene transcripts including those of the PU.1 gene. Oncogene. 1998; 17:2287–2293. [PubMed: 9811459]

23. Kim I, Yilmaz OH, Morrison SJ. CD144 (VE-cadherin) is transiently expressed by fetal liver hematopoietic stem cells. Blood. 2005; 106:903–905. [PubMed: 15831702]
24. Taoudi S, et al. Progressive divergence of definitive haematopoietic stem cells from the endothelial compartment does not depend on contact with the foetal liver. Development. 2005; 132:4179–4191. [PubMed: 16107475]
25. Ichikawa M, et al. AML-1 is required for megakaryocytic maturation and lymphocytic differentiation, but not for maintenance of hematopoietic stem cells in adult hematopoiesis. Nat Med. 2004; 10:299–304. [PubMed: 14966519]
26. Growney JD, et al. Loss of Runx1 perturbs adult hematopoiesis and is associated with a myeloproliferative phenotype. Blood. 2005; 106:494–504. [PubMed: 15784726]
27. Monvoisin A, et al. VE-cadherin-CreERT2 transgenic mouse: a model for inducible recombination in the endothelium. Dev Dyn. 2006; 235:3413–3422. [PubMed: 17072878]
28. Bertrand JY, et al. Characterization of purified intraembryonic hematopoietic stem cells as a tool to define their site of origin. Proc Natl Acad Sci U S A. 2005; 102:134–139. [PubMed: 15623562]
29. Chung JH, Whiteley M, Felsenfeld G. A 5' element of the chicken beta-globin domain serves as an insulator in human erythroid cells and protects against position effect in Drosophila. Cell. 1993; 74:505–514. [PubMed: 8348617]
30. Inman KE, Downs KM. Brachyury is required for elongation and vasculogenesis in the murine allantois. Development. 2006; 133:2947–2959. [PubMed: 16835439]

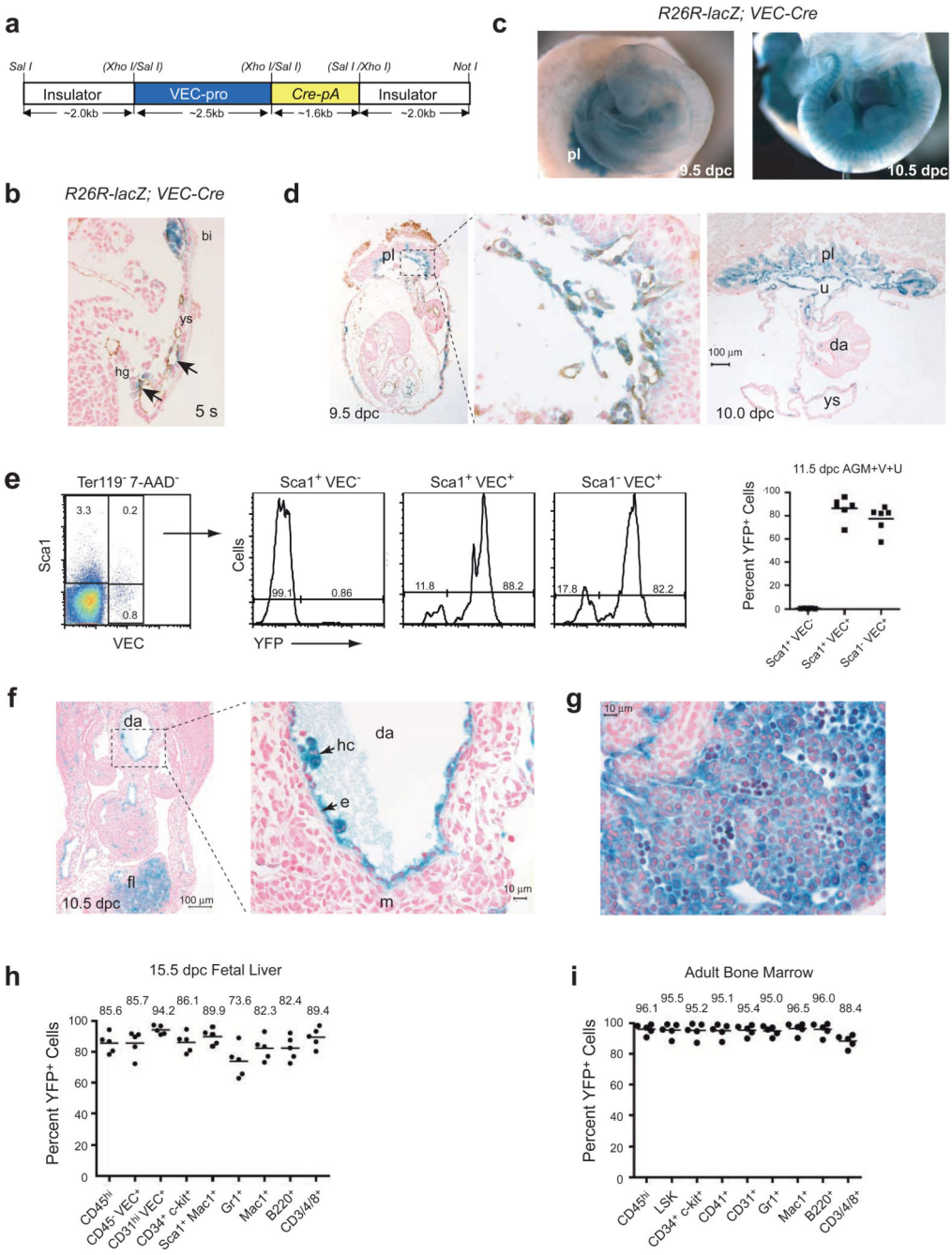

Figure 1. VEC-Cre excision marks endothelium and blood

a. Schematic diagram of the VEC-Cre transgene. The VEC promoter (VEC-pro) and Cre plus polyA tail (Cre-pA) were flanked by insulator sequences from the chicken γ-globin gene.

b. Sagittal section of a 5 s *R26R-lacZ;VEC-Cre* conceptus near the hindgut(hg). Arrows indicate β-gal$^+$ (blue) PECAM1$^+$ (brown) vitelline vasculature. ys, yolk sac; bi, blood island. The blood island contains β-gal$^+$ primitive erythrocytes derived from yolk sac mesoderm in which VEC-Cre was active.

c. Whole mount conceptuses showing β-gal activity in the embryonic vasculature and placenta (pl).

d. VEC-Cre excision in placenta and umbilical artery endothelium. Left panel is from a 9.5 dpc conceptus. Detail of boxed region in placental labyrinth is to the right. β-gal$^+$ cells are blue and PECAM1$^+$ cells are brown. On the far right is a transverse section through a 10.0 dpc *R26R-lacZ;VEC-Cre* conceptus with abundant β-gal$^+$ endothelial cells in the placenta (pl) and umbilical artery (u). da, dorsal aorta; ys, yolk sac.

e. FACS analysis of cells from the AGM region, vitelline and umbilical arteries of 11.5 dpc *R26R-YFP;VEC-Cre* conceptuses stained for Sca1, VEC, Ter119, and 7-AAD. Gated populations in scatter plot were analyzed for YFP in histograms to the right. Graph shows percent of YFP$^+$ cells in each subpopulation, line indicates mean. Non-hematopoietic, non-endothelial cells (Sca1$^+$ VEC$^-$) are YFP$^-$. Means (± SD) for each population are: Sca1$^+$ VEC$^-$ (0.7 ± 0.2); Sca1$^+$ VEC$^+$ (86.4 ± 9.9); Sca1$^-$VEC$^+$ (77.4 ± 11.1).

f. On left is a transverse section through the AGM region of a 10.5 dpc conceptus. Detail on right is from boxed region showing β-gal$^+$ endothelial cells (e) and hematopoietic clusters (hc) in the dorsal aorta (da). Note that the sub-aortic mesenchyme (m) is β-gal$^-$. fl, fetal liver.

g. β-gal$^+$ cells in the liver of *R26R-lacZ;VEC-Cre* fetuses (10.5 dpc).

h. Percentage of YFP$^+$ fetal liver cells of multiple cell surface phenotypes (gated from Ter119$^-$ 7-AAD$^-$ cells) from 15.5 dpc *R26R-YFP;VEC-Cre* conceptuses. Mean ± SD for each population: CD45^{hi} (85.6 ± 6.3); CD45$^-$ VEC$^+$ (85.7 ± 8.2); CD31^{hi} VEC$^+$ (94.2 ± 2.8); CD34$^+$ c-kit$^+$ (86.1 ± 6.4); Sca1$^+$ Mac1$^+$ (89.9 ± 5.1); Gr1$^+$ (73.6 ± 10.3); Mac1$^+$ (82.3 ± 7.6); B220$^+$ (82.4 ± 7.9); CD3/4/8$^+$ (89.4 ± 6.4).

i. Percentage of YFP$^+$ bone marrow cells (gated from Ter119$^-$ 7-AAD$^-$ cells) in *R26R-YFP;VEC-Cre* adult mice. CD45^{hi} (96.1 ± 3.3); LSK (95.5 ± 4.4); CD34$^+$ c-kit$^+$ (95.2 ± 4.9); CD41$^+$ (95.1 ± 4.9); CD31$^+$ (95.4 ± 3.5); Gr1$^+$ (95.0 ± 3.2); Mac1$^+$ (96.5 ± 3.6); B220$^+$ (96.0 ± 4.2); CD3/4/8$^+$ (88.4 ± 4.1).

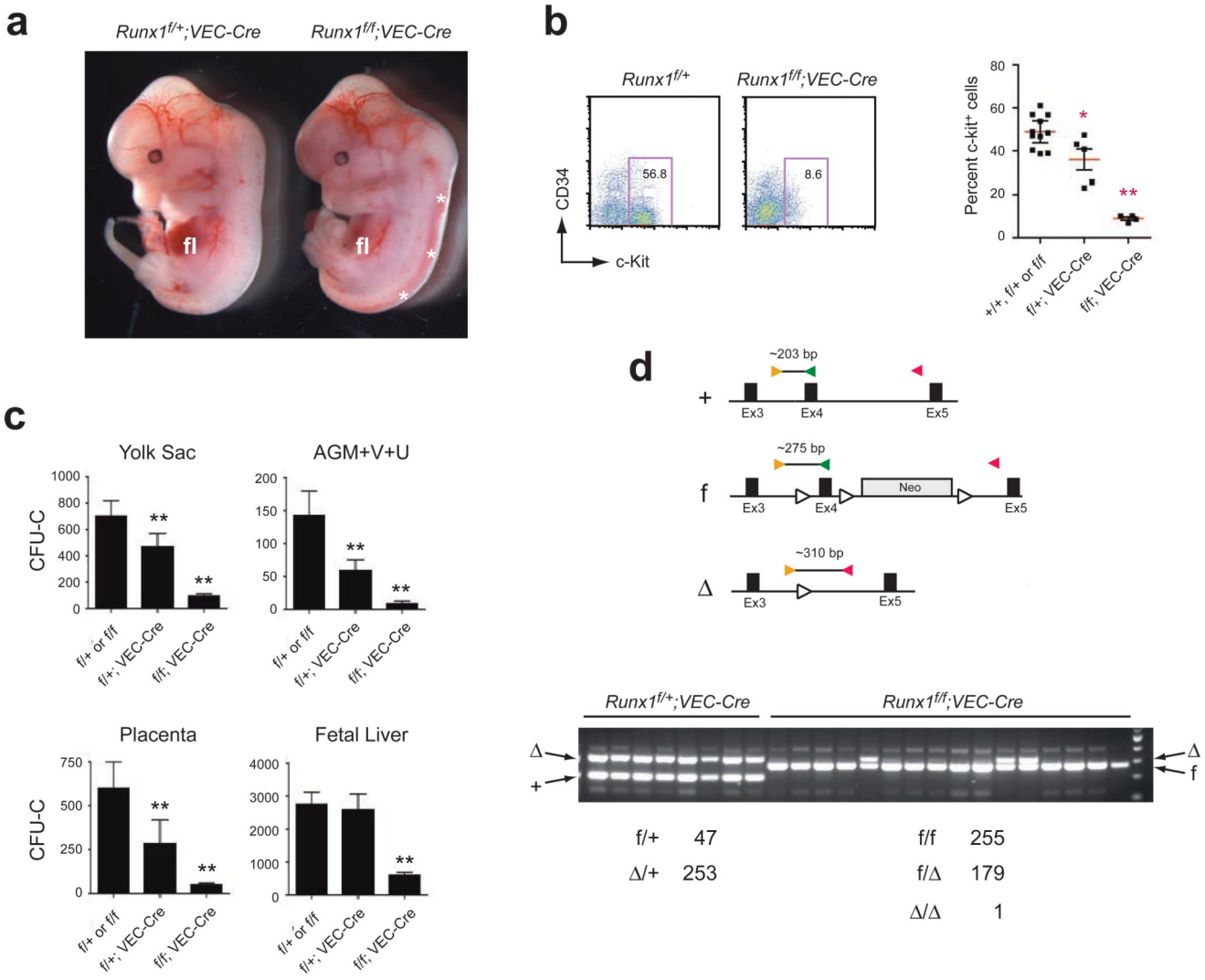

Figure 2. Runx1 is required in VEC$^+$ cells for hematopoietic progenitor formation

a. Gross appearance of *Runx1$^{f/f}$;VEC-Cre* fetuses. Note the central nervous system hemorrhaging (white asterisks) and pale fetal liver (fl). VEC-Cre deletion of Runx1 resulted in the same phenotype as germline Runx1 deletion, but the penetrance was lower.

b. FACS analysis of Ter119$^-$ 7-AAD$^-$ cells from 11.5 dpc fetal livers. Error bars in plot on right represent 95% confidence intervals. Significant differences from combined +/+, f/+, and f/f samples are indicated with asterisks (*P = 0.05, **P = 0.01; ANOVA and Dunnett's multiple comparison test).

d. CFU-C assays of yolk sac, combined AGM region, umbilical and vitelline arteries (AGM +U+V), placenta, and fetal liver (represented as numbers per embryo equivalent, error bars indicate 95% confidence intervals). Significant differences from *Runx1$^{f/f}$* or *Runx1$^{f/+}$* conceptuses are indicated with asterisks (**P = 0.01). Data are averaged from 16 litters, with 10 – 31 animals per genotype.

d. PCR genotyping of single colonies picked from CFU-C assays. On top is shown locations of the three primers (colored triangles) used to detect the wildtype (+), floxed (f), and

deleted (Δ) *Runx1* alleles. LoxP sites are open triangles. The combined number of colonies from 11.5 dpc AGM+V+U and fetal livers of each genotype are indicated below the gel. Since Runx1 haploinsufficiency decreases the number of CFU-Cs [18], the percentage of $Runx1^{f/\Delta}$ colonies may actually underestimate the excision frequency.

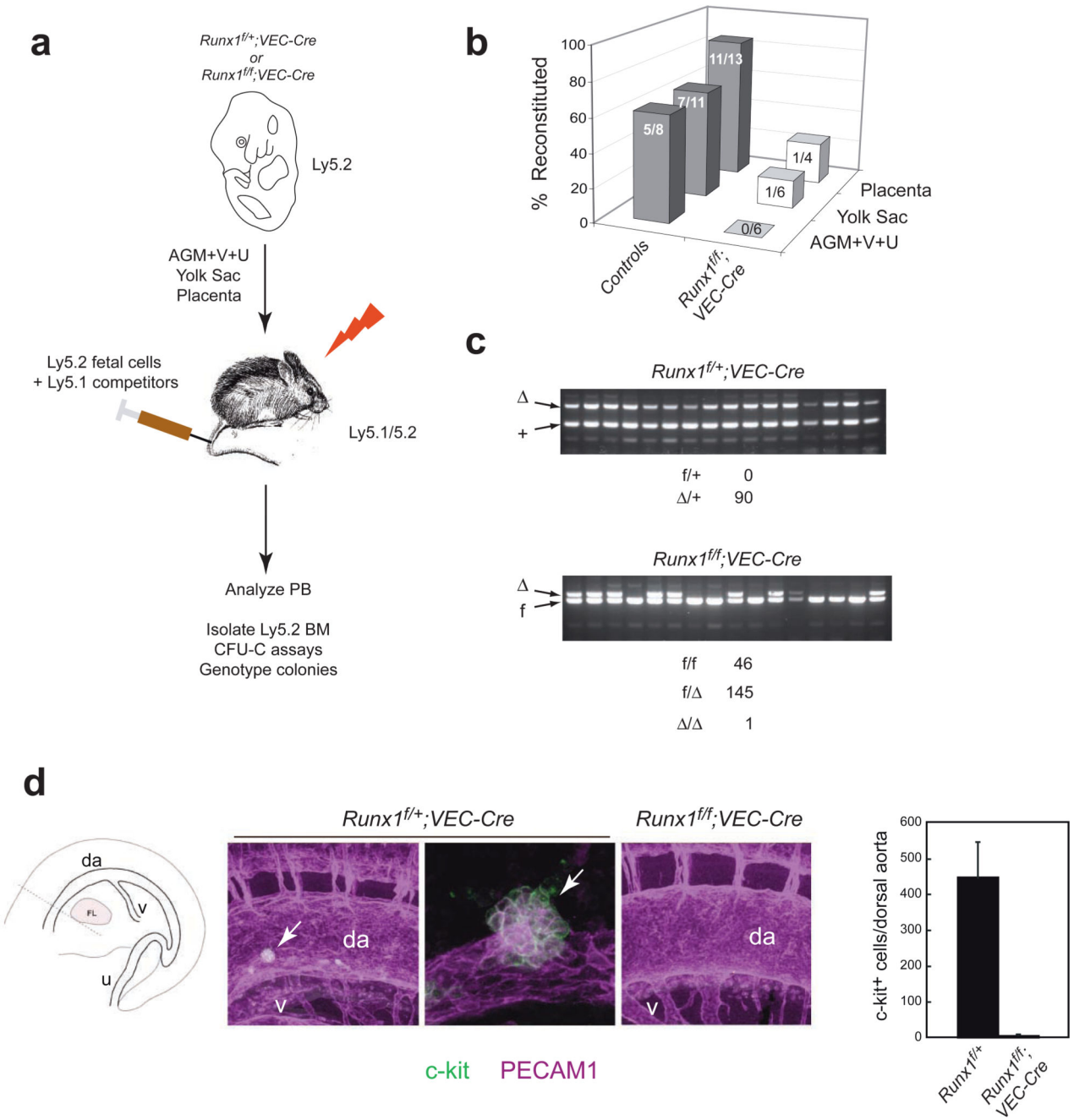

Figure 3. Runx1 is required in VEC$^+$ cells for HSC emergence

a. Scheme of transplantations and analyses. Donor derived cells were isolated from transplant recipients and plated in methylcellulose assays, and individual colonies were genotyped.

b. Engraftment as assessed by FACS on peripheral blood to detect donor derived (Ly5.1$^-$/5.2$^+$) cells. Numbers indicate successfully reconstituted recipients (>5% donor-derived cells) per number transplanted. Mice were transplanted with one embryo equivalent

of 11.5 dpc fetal cells from each site. Control samples are from *Runx1*$^{f/f}$, *Runx1*$^{f/+}$ and *Runx1*$^{f/+}$*;VEC-Cre* conceptuses.

c. PCR genotyping of single colonies picked from CFU-C assays of donor-derived placenta cells sorted from the bone marrow of transplant recipients. The number of colonies of each genotype is indicated below the gel.

d. Confocal images of the caudal region of 10.5 dpc embryos (35–36 s) stained with antibodies to PECAM1 (pink) and c-kit (green). Diagram on left illustrates area analyzed (da, dorsal aorta; v, vitelline artery; u, umbilical artery). Arrow indicates a c-kit^{+} cluster in the ventral aspect of the dorsal aorta. On right is a bar graph representing the number of c-kit^{+} cells in the dorsal aorta from three embryos of each genotype. Error bars represent standard deviation.

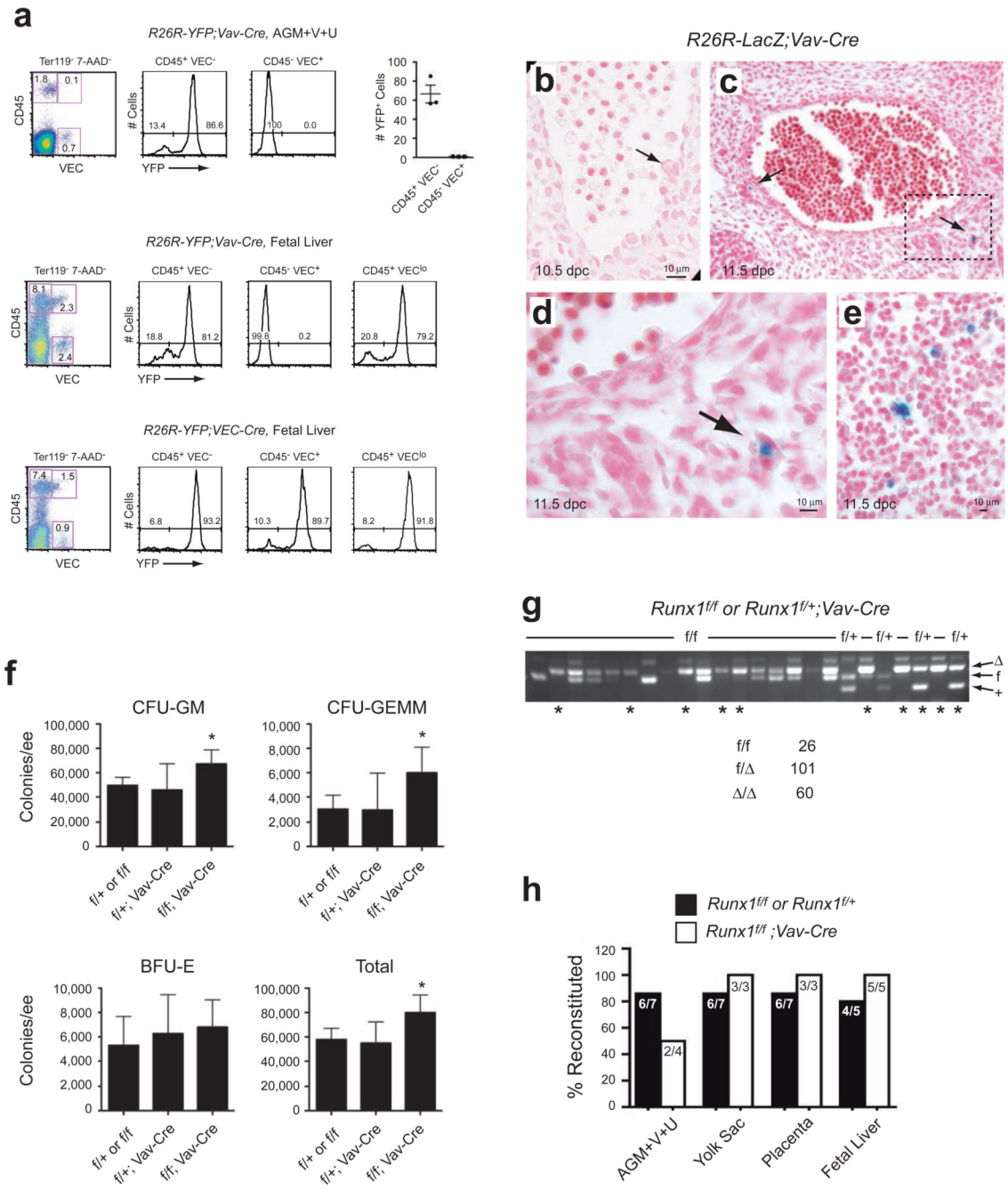

Figure 4. Runx1 is not required in Vav^{+} cells for CFU-C or HSC emergence

a. Flow cytometric assay of AGM region, vitelline and umbilical arteries (AGM+V+U) and fetal livers from 11.5 dpc *R26R-YFP;Vav-Cre* conceptuses demonstrating deletion in blood but not in endothelium. Scatter plot shows 7AAD^{-} Ter119^{-} cells gated and analyzed for CD45 and VEC expression. Histograms to the right represent the percent of YFP positive cells (± SEM) in each of the gated populations. The CD45^{+}VEC^{+} population from the AGM +V+U was too small to analyze for YFP expression. Graph on far right in top row shows mean ± SEM for AGM+V+U. Activation of the *R26R-YFP* allele in both fetal liver

endothelium ($CD45^{-}$ VEC^{+}) and blood ($CD45^{+}$ VEC^{-} and $CD45^{+}$ VEC^{+}) with VEC-Cre is shown at the bottom for comparison.

b. Dorsal aorta from the AGM region of a 10.5 dpc *R26R-lacZ;Vav-Cre* conceptus. Arrow points to an intra-aortic cluster, all of which are $\beta\text{-gal}^{-}$.

c. Transverse section through the dorsal aorta of an 11.5 dpc *R26R-lacZ;Vav-Cre* conceptus. Arrows indicate two $\beta\text{-gal}^{+}$ cells in the subaortic mesenchyme.

d. Detail of $\beta\text{-gal}^{+}$ cell in the subaortic mesenchyme from boxed region in c.

e. $\beta\text{-gal}^{+}$ cells in the fetal liver (11.5 dpc).

f. CFU-C assays from 15.5 dpc fetal livers. Asterisks indicate significant differences from f/+ or f/f animals ($P = 0.05$, ANOVA and Dunnett's multiple comparison test). Data are compiled from 3–8 conceptuses of each genotype. Error bars represent 95% confidence intervals.

g. PCR genotyping of colonies from CFU-C assays. The gel is from 11.5 dpc AGM+V+U colonies. Horizontal lines above lanes are *Runx1*$^{f/f}$*;Vav-Cre* colonies, and *Runx1*$^{f/+}$*;Vav-Cre* colonies are labeled f/+. Asterisks indicate colonies in which both *Runx1*^{f} alleles (or in the case of *Runx1*$^{f/+}$*;Vav-Cre* colonies, one *Runx1*^{f} allele) were completely deleted. Numbers below the gel represent total colonies from 11.5 dpc tissues (AGM+V+U, yolk sac, placenta, fetal liver).

h. Engraftment of 11.5 dpc tissues (1 ee) as assessed by FACS on peripheral blood to detect donor derived ($Ly5.1^{-}/5.2^{+}$) cells. Numbers within bars indicate successfully reconstituted recipients/number transplanted.